

Nodal Structure of Quasi-Two-Dimensional Superconductors Probed by a Magnetic Field

A. Vorontsov and I. Vekhter

Department of Physics and Astronomy, Louisiana State University, Baton Rouge, Louisiana, 70803, USA
(Received 16 January 2006; published 12 June 2006)

We consider a quasi-two-dimensional superconductor with line nodes in the presence of an in-plane magnetic field, and compute the dependence of the specific heat C and the in-plane heat conductivity κ on the angle between the field and the nodal direction in the vortex state. We use a variation of the microscopic Brandt-Pesch-Tewordt method that accounts for the scattering of quasiparticles off vortices, and analyze the signature of the nodes in C and κ . At low to moderate fields the specific heat anisotropy changes sign with increasing temperature. Comparison with measurements of C and κ in CeCoIn₅ resolves the contradiction between the two in favor of the $d_{x^2-y^2}$ gap.

DOI: 10.1103/PhysRevLett.96.237001

PACS numbers: 74.25.Fy, 74.20.Rp, 74.25.Bt

Introduction.—Remarkable properties of superconductors below the transition temperature, T_c , are due to formation of the Cooper pairs and opening of the energy gap in the single particle spectrum. The structure of the gap is intimately related to the nature of the pairing interaction, and therefore its experimental determination is very important. In simple metals the phonon-mediated electron attraction and the gap are isotropic around the Fermi surface. In contrast, in many recently discovered superconductors the gap is anisotropic, and often vanishes (has nodes) for selected directions in the momentum space.

While the existence and topological structure (line vs point) of gap nodes can be inferred from the power laws in the temperature dependence of the thermodynamic and transport properties, experimental determination of the nodal *directions* is more challenging. Currently the most widely used probes utilize an applied magnetic field, \mathbf{H} , as a directional probe of unpaired quasiparticles (QP).

Low-energy quasiparticles only exist in the near-nodal regions. They are excited by the applied field, predominantly at the nodes where the QP velocity is normal to \mathbf{H} . Consequently, the QP density changes with the relative orientation of the field with respect to the nodes. It was predicted that the low-energy density of states (DOS), and the electronic specific heat, C , have minima when the magnetic field is aligned with the nodes [1].

Because of challenges in measuring the electronic contribution to $C(T, \mathbf{H})$, experimental results exist only for a few materials [2,3]. The anisotropy of the electronic thermal conductivity, $\kappa_{xx} \equiv \kappa$, under a rotating field is easier to measure, and it was determined in several systems [4–6]. The orientational dependence of the in-plane $\kappa(\mathbf{H})$ is more complex than that of the specific heat as it combines the anisotropy due to nodal structure with that due to the difference in scattering normal to and parallel to the vortices. Theoretical interpretation of the anisotropy of transport properties proved elusive as the existing theories have difficulties accounting for the two modulations, and cannot unequivocally determine whether a local minimum or a maximum occurs when the field is along a node. Consequently, more theoretical work is needed to examine the

experimentally conjectured gap anisotropy [5,6]. Moreover, in heavy fermion CeCoIn₅, where data on both C and κ anisotropy exist, the conclusions appear contradictory: d_{xy} ($d_{x^2-y^2}$) gap symmetry was inferred from C (κ) [3,6].

In most approaches the effect of \mathbf{H} on the QPs is included via the Doppler energy shift due to supercurrents around the superconducting vortices [7], and the QP lifetime is not affected directly [8]. In reality, vortices scatter quasiparticles carrying the heat current and not just shift their energy. Consequently, the behavior of $\kappa(T, \mathbf{H})$ is determined by the competition between the enhancement of the DOS and the vortex scattering. There are indications that vortex scattering affects transport already at moderate, compared to the upper critical field H_{c2} , fields [9,10], but its effect for the in-plane field and on the anisotropy in $C(\mathbf{H})$ and $\kappa(\mathbf{H})$ has not been studied.

In this Letter we present a unified microscopic approach to computing the anisotropy of thermodynamic and transport properties of nodal superconductors in the vortex state at moderate to high magnetic field. We apply the method to quasi-two-dimensional superconductors with line nodes, and consider the field rotated in the xy plane. We are able to account for both twofold and fourfold variations of $\kappa(T, \mathbf{H})$ with angle. For $d_{x^2-y^2}$ gap, the competition between the *transport* scattering rate and the DOS leads to switching from minima to maxima for \mathbf{H} along the nodes in the fourfold part of $\kappa(T, \mathbf{H})$ upon increasing temperature. We find that, due to the field dependence of the *single particle* lifetime, the minima and the maxima in the specific heat also switch at higher T and H . Hence in a wide T - H range the maxima (rather than minima) in $C(T, \mathbf{H})$ indicate a nodal direction. Our results for the $d_{x^2-y^2}$ gap are in a semiquantitative agreement with experiment on CeCoIn₅.

Model and approach.—We consider a quasi-two-dimensional system with a model Fermi surface (FS) $p_f^2 = p_x^2 + p_y^2 - (r^2 p_f^2) \cos(2s p_z / r^2 p_f)$. The parameters, r and s , determine the corrugation along the z axis and the ratio $v_{f,z} / v_{f,\perp}$ (at $p_x^2 + p_y^2 = p_f^2$), respectively. We assume a separable pairing interaction, $V(\hat{\mathbf{p}}, \hat{\mathbf{p}}') = V_0 \mathcal{Y}(\hat{\mathbf{p}}) \mathcal{Y}(\hat{\mathbf{p}}')$,

where $\mathcal{Y}(\hat{\mathbf{p}})$ are the normalized basis functions for the angular momentum eigenstates, so that $\mathcal{Y}(\hat{\mathbf{p}}) = \sqrt{2} \times \cos 2\phi_{\hat{p}}$ [$\mathcal{Y}(\hat{\mathbf{p}}) = \sqrt{2} \sin 2\phi_{\hat{p}}$] for $d_{x^2-y^2}$ (d_{xy}) gap. Here $\phi_{\hat{p}}$ is the angle between the projection of the momentum \mathbf{p} onto the xy plane and the x axis. The field, \mathbf{H} , is in the xy plane, at an angle ϕ_0 to the x axis. We choose r, s so that the normal state transport anisotropy is moderate, and the vortex state is Abrikosov-like. We consider $H \gg H_{c1}$ when the field inside the superconductor is essentially uniform. We also ignore Zeeman splitting.

We rotate x and y axes around z to choose the field direction as the new x axis, and model the spatial dependence of superconducting order parameter by an Abrikosov-like solution, $\Delta(\mathbf{R}, \hat{\mathbf{p}}) = \Delta(\mathbf{R})\mathcal{Y}(\hat{\mathbf{p}})$, where $\Delta(\mathbf{R}) =$

$$\left[-2i\tilde{\varepsilon} + \mathbf{v}_f(\hat{\mathbf{p}}) \left(\nabla_{\mathbf{R}} - i \frac{2e}{\hbar c} \mathbf{A}(\mathbf{R}) \right) \right] f^R(\hat{\mathbf{p}}, \mathbf{R}; \varepsilon) = 2\tilde{\Delta} i g^R(\hat{\mathbf{p}}, \mathbf{R}; \varepsilon). \quad (1)$$

Here $\tilde{\varepsilon} = \varepsilon - \Sigma^R(\mathbf{R}; \varepsilon)$, $\tilde{\Delta} = \Delta(\hat{\mathbf{p}}, \mathbf{R}) + \Delta_{\text{imp}}^R$, and we treat the self-energies Σ^R , Δ_{imp}^R due to impurity scattering in the self-consistent T -matrix approximation, and focus here on the unitarity limit (scattering phase shift $\pi/2$) for clean systems (normal state scattering rate $\Gamma \ll T_c$). The normal electron Green's function $g^R(\hat{\mathbf{p}}, \mathbf{R}; \varepsilon)$ is determined via the normalization condition $(g^R)^2 - \underline{f}^R \underline{f}^R = -\pi^2$, where $\underline{f}^R(\hat{\mathbf{p}}, \mathbf{R}; \varepsilon) = f^R(-\hat{\mathbf{p}}, \mathbf{R}; -\varepsilon)^*$. Equation (1) is complemented by the self-consistency condition for Δ .

To solve the equations we make use of the approximation due to Brandt, Pesch, and Tewordt (BPT) [16], and replace $g^R(\mathbf{R}, \hat{\mathbf{p}}, \varepsilon)$, by its spatial average. If \mathbf{K} is a vector of the reciprocal vortex lattice, the Fourier components $g^R(\mathbf{K}) \propto \exp(-\Lambda^2 \mathbf{K}^2)$, hence the spatial average $\mathbf{K} = 0$ dominates [16]. The method is nearly exact at $H \lesssim H_{c2}$, but gives semiquantitatively correct results down to much lower fields. In extreme type-II [17], and in the nodal superconductors [9,18] the method remains valid over almost the entire range $H_{c1} \ll H < H_{c2}$ [19], and was used to study unconventional superconductors in the vortex state [9,11,21].

With averaged g^R we solve Eq. (1) by expanding Δ , f^R , \underline{f}^R in the orthonormal set $\{|\mathbf{R}\rangle|n\rangle\}$, and using the ladder operators for the oscillator states, a and a^\dagger [11,20], to rewrite $\mathbf{v}_f(\hat{\mathbf{p}}) [\nabla_{\mathbf{R}} - i(2e/\hbar c)\mathbf{A}(\mathbf{R})] = v_- a - v_+ a^\dagger$, where $v_\pm = [v_z/\sqrt{s} \pm i v_y \sqrt{s}]/(\Lambda\sqrt{2})$. Lengthy but straightforward calculation gives the closed form expressions for functions f^R , \underline{f}^R , and g^R for a set Δ_n , which is then determined self-consistently. For $n = 0$ only we find

$$g^R(\hat{\mathbf{p}}; \varepsilon) = \frac{-i\pi}{\sqrt{1 - i\sqrt{\pi} \left(\frac{2\Lambda\Delta_0}{|\tilde{v}_f^\perp|} \right)^2 \mathcal{Y}^2(\hat{\mathbf{p}}) W \left(\frac{2\varepsilon\Lambda}{|\tilde{v}_f^\perp|} \right)}}, \quad (2)$$

similar to Refs. [9,11]. Here $W(z) = \exp(-z^2)\text{erfc}(-iz)$, and the dependence on the field direction is via the rescaled component of the Fermi velocity normal to \mathbf{H} , $|\tilde{v}_f^\perp(\mathbf{p}_f)|^2 = v_{f,z}^2/s + s v_{f,y}^2$. The expression for arbitrary

$\sum_n \Delta_n \langle \mathbf{R} | n \rangle$. Here $\langle \mathbf{R} | n \rangle = \sum_{k_y} C_{k_y}^{(n)} \Phi_n[(z - \Lambda^2 k_y)/\sqrt{s}\Lambda] \times \exp(ik_y y)$, $\Phi_n(z)$ is the eigenfunction of the n th state of a harmonic oscillator, $\Lambda^2 = \hbar c/2eH$, and normalized $C_{k_y}^{(n)}$ ($\sum_{k_y} |C_{k_y}^{(n)}|^2 = 1$) determine the structure of the vortex lattice. The factor \sqrt{s} ensures that Φ_n are the solutions to the linearized equations for the order parameter [11,12], and Δ_n is the amplitude of the n th component. In s -wave superconductors the vortex state is a superposition of $n = 0$ states only; however, for singlet pairing in the higher angular momentum channels the self-consistency requires admixture of other even n [13,14]. We use $n = 0, 2, 4$, since inclusion of higher n does not alter the results.

We use the quasiclassical Green's function approach [15], where the equation for the retarded (index R) anomalous (Gor'kov) Green's function, is given by

n has a similar structure, but involves combinations of Δ_n and higher derivatives of $W(z)$ [12].

The density of states (DOS) is $N(T, H; \varepsilon)/N_f = (-1/\pi) \int d\hat{\mathbf{p}}_f \Im \text{mg}^R(\hat{\mathbf{p}}; \varepsilon)$, where N_f is the normal state DOS per spin at the Fermi level. From the DOS we determined the entropy, $S(T, H)$, computed the specific heat, $C = T \partial S / \partial T$, by numerical differentiation, and verified that far from the transition $T_c(H)$ the expression

$$C(T, H) = \frac{1}{2} \int_{-\infty}^{+\infty} d\varepsilon \frac{\varepsilon^2 N(T, H; \varepsilon)}{T^2 \cosh^2(\varepsilon/2T)}, \quad (3)$$

gives accurate results. We use Eq. (3) below.

The thermal conductivity tensor can be obtained using the Keldysh technique [12], and has a particularly simple form for the Born and unitarity scattering limits [22,23]

$$\frac{\kappa_{ij}(T, H)}{T} = \int_{-\infty}^{+\infty} \frac{d\varepsilon}{2T} \frac{\varepsilon^2}{T^2} \cosh^{-2} \frac{\varepsilon}{2T} \times \int d\hat{\mathbf{p}} v_{f,i} v_{f,j} N(T, H; \hat{\mathbf{p}}, \varepsilon) \tau_H(T, H; \hat{\mathbf{p}}, \varepsilon). \quad (4)$$

Here N is the angle-dependent DOS, and τ_H has the meaning of the *transport* lifetime due to both impurity and vortex scattering. For the $n = 0$ channel [9,11,24],

$$\frac{1}{2\tau_H} = -\Im \Sigma^R + \frac{2\sqrt{\pi} \Lambda \Delta_0^2 \mathcal{Y}^2}{|\tilde{v}_f^\perp|} \frac{\Im [g^R W(2\varepsilon\Lambda/|\tilde{v}_f^\perp|)]}{\Im \text{mg}^R},$$

and addition of other channels results in a more complex combination of the W function and its derivatives [12].

Results.—We show the results for $s = 0.5$, $r = 0.5$, which gives $H_{c2}^{ab}/H_{c2} \approx 2.45$ similar to CeCoIn₅, and for $\Gamma/(2\pi T_c) = 0.007$ [25]. The main qualitative difference from previous results is already clear from the behavior of the DOS shown in Fig. 1(a). In the Doppler shift method the DOS anisotropy, $N(\varepsilon, \mathbf{H} \parallel \text{antinode}) - N(\varepsilon, \mathbf{H} \parallel \text{node})$, increases as \sqrt{H} at $\varepsilon = 0$, and vanishes at $\varepsilon \sim$

$v_F\sqrt{s}/\Lambda$ [1,26]. In contrast, the anisotropy in the residual ($\varepsilon = 0$) DOS has a maximum at $H \sim 0.1H_{c2}$, and *reverses* above the field $H \sim 0.5H_{c2}$. Below this field the anisotropy also *changes sign* at a finite $\varepsilon(H)$, see Fig. 1(a).

Since $W(z)$ and its derivatives in Eq. (2) are complex functions, our $N(\varepsilon)$ cannot be obtained from the BCS DOS by a simple energy shift: there is an anisotropic single particle scattering rate due to scattering from vortices (vanishingly small along \mathbf{H} , largest normal to \mathbf{H}). This occurs since in the BPT method g^R is averaged incoherently in different unit cells of the vortex lattice. Vortex scattering is pair breaking, and hence enhances the DOS.

Consider the contribution to the DOS from different FS regions and focus first on $\varepsilon = 0$, Figs. 1(b) and 1(c). At low fields the vortex scattering rate is small, and the unpaired states emerge only near the nodes. When $\mathbf{H} \parallel$ node the number of such states at the nodes aligned with the field is small, while $\mathbf{H} \parallel$ antinode produces states at all nodes, see Fig. 1(c), and $N(0, \mathbf{H} \parallel \text{antinode}) > N(0, \mathbf{H} \parallel \text{node})$ as in the Doppler shift method [1]. At higher fields the pair breaking is stronger, and, for $\mathbf{H} \parallel$ antinode, it generates the unpaired states in all directions on the FS *except* close to the field direction, see Fig. 1(b). For $\mathbf{H} \parallel$ node the field-induced states appear everywhere on the FS [Fig. 1(b)], leading to the anisotropy reversal [27].

Now consider $0 < \varepsilon \ll \Delta_0$, Fig. 1(d). In a pure system at zero field the dominant contribution to $N(\varepsilon)$ is from sharp peaks at directions $\hat{\mathbf{p}}_\varepsilon$, close to the nodes, such that $|\Delta(\hat{\mathbf{p}}_\varepsilon)| = \varepsilon$. Scattering redistributes the spectral weight from the peak. Vortex scattering at $\hat{\mathbf{p}}_\varepsilon$, increases with H , and is stronger for $\mathbf{H} \perp \hat{\mathbf{p}}_\varepsilon$ than for $\mathbf{H} \parallel \hat{\mathbf{p}}_\varepsilon$. For $\varepsilon > \varepsilon(H)$ $\mathbf{H} \parallel$ node fills the near-nodal states, but does not broaden the peak nearest to $\hat{\mathbf{p}}_\varepsilon$ significantly, Fig. 1(d). For $\mathbf{H} \parallel$ antinode most of the weight in the peak is shifted away. This leads to a higher DOS at $\varepsilon > \varepsilon(H)$ for the field along the node, see Fig. 1(a).

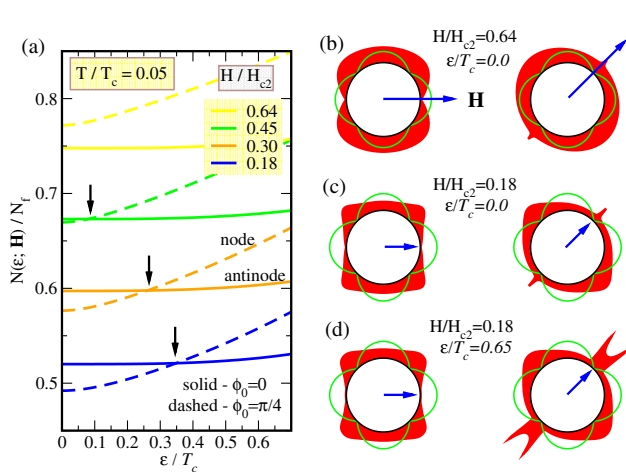


FIG. 1 (color online). (a) Low-energy DOS for $\mathbf{H} \parallel$ antinode and $\mathbf{H} \parallel$ node at $T = 0.05T_c$. Arrows indicate $\varepsilon(H)$, see text. (b)–(d) Angle-resolved DOS plotted at each position on the FS. Net DOS is proportional to the red shaded area, see text.

Figure 2 shows the specific heat anisotropy. The dominant contribution to $C(T, \mathbf{H})$ is from the DOS at energies $\varepsilon \sim 2.4 T$, see Eq. (3). Therefore even at low fields, when $N(0, \mathbf{H} \parallel \text{antinode}) > N(0, \mathbf{H} \parallel \text{node})$, the anisotropy of the specific heat is reversed at $T_0 \sim 0.1\text{--}0.2T_c$ [28]. Below T_0 , $C(T, \mathbf{H})$ has a minimum when the field is applied along a nodal direction, while at higher T it has a *maximum* for this field orientation. At higher fields \mathbf{H} along a node gives a maximum in the angle-dependent specific heat at all but the lowest T . This result directly affects the experimental determination of the nodal directions.

The measurements on CeCoIn₅ were carried out for $0.18 \leq H/H_{c2} \leq 0.5$, and for $T > 0.1T_c$ [3]. For this system H_{c2} is Pauli limited [29], and the orbital critical field, $H_{c2}^{(\text{orb})}$, may be as high as $2.5H_{c2}$. We find that $T_0(H)$ in Fig. 2 is weakly field dependent for $0.1 \leq H/H_{c2}^{(\text{orb})} \leq 0.3$. Therefore our results indicate that maxima, rather than minima in $C(T, \mathbf{H})$ occur for $\mathbf{H} \parallel$ node in this regime, and the data of Ref. [3] support the $d_{x^2-y^2}$ gap symmetry (rather than the d_{xy} order inferred by the authors from the low T , low H theory [1]). While the BPT approach likely overestimates the vortex scattering at low H/H_{c2} , the extended range of this shape of $C(T, \mathbf{H})$ is also in favor of $d_{x^2-y^2}$ pairing.

This conclusion is supported by the analysis of the thermal conductivity, shown in Fig. 3 for the heat current $\mathbf{j}_q \parallel \hat{\mathbf{x}}$. Comparison can be made with $\kappa(T, \mathbf{H})$ as shown in Ref. [6] for $T \leq 0.5T_c$ and fields $H \leq 0.3H_{c2}$. In this range we find the overall shape of the curve and the amplitude of the peak ($\sim 1\text{--}3\%$) at the nodal angle always similar to those in the right panel Fig. 3. We also confirmed that d_{xy} gap is inconsistent with the results of Ref. [6]. The orientational dependence of $C(T, \mathbf{H})$ for the d_{xy} gap is obtained by a 45° degree rotation in Fig. 2. In contrast, the variation of $\kappa(T, \mathbf{H})$ with angle is different for the two cases since the

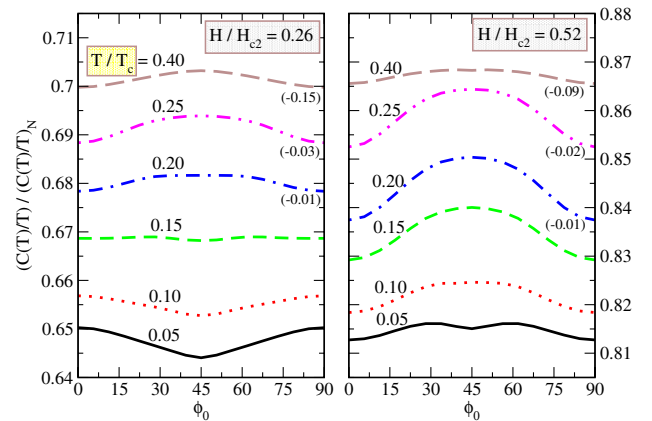


FIG. 2 (color online). Specific heat anisotropy for different T at two fields. Nodal direction $\phi_0 = 45^\circ$. Left panel: $H = 0.26H_{c2}$, inversion of the anisotropy occurs at $T_0 \sim 0.15T_c$. Right panel: $H = 0.52H_{c2}$, no minimum for the field along the node at any T . Some curves are shifted by the amount indicated in parentheses.

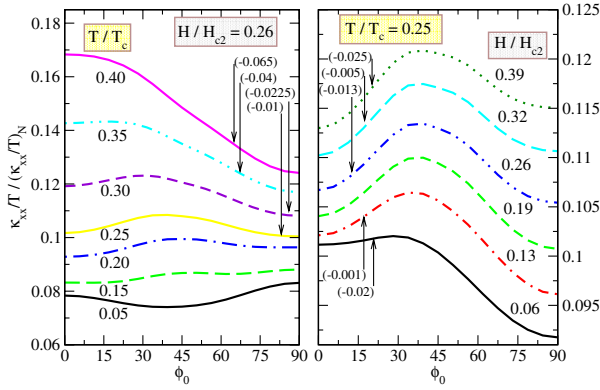


FIG. 3 (color online). Thermal conductivity anisotropy for different T at $H = 0.26H_{c2}$ (left panel), and for different H at $T = 0.25T_c$ (right panel). Curves are shifted for clarity by the amount indicated. Left panel: notice the reversal of the 0° – 90° anisotropy and the change from minimum to maximum at 45° . Right panel provides direct comparison with Ref. [6].

heat current $\mathbf{j}_q \parallel \hat{\mathbf{x}}$ is along the antinodal (nodal) direction for the $d_{x^2-y^2}$ (d_{xy}) gap [12].

The fourfold angle dependence of $\kappa(\mathbf{H})$ is superimposed on the twofold variation due to relative orientation of \mathbf{j}_q and \mathbf{H} . The field is strongly pairbreaking for $\hat{\mathbf{p}} \perp \mathbf{H}$, and QPs which contribute the most to $\kappa(T, \mathbf{H})$, are created for $\mathbf{H} \perp \mathbf{j}_q$ [30]. Consequently, at low T , $\kappa(T, \mathbf{H} \perp \mathbf{j}_q) > \kappa(T, \mathbf{H} \parallel \mathbf{j}_q)$. At higher T the QP are thermally excited, and $\kappa(T, \mathbf{H} \perp \mathbf{j}_q) < \kappa(T, \mathbf{H} \parallel \mathbf{j}_q)$ due to vortex scattering, see Fig. 3. $\kappa(T, \mathbf{H} \parallel \text{node})$ has a local minimum at low T, H , but develops a maximum at higher T . At yet higher T , $\kappa(T, \mathbf{H})$ is essentially twofold.

Conclusions.—We developed a fully self-consistent microscopic calculation of the magnetic field-induced anisotropy of thermal and transport properties of nodal superconductors. We applied the method to quasi-two-dimensional systems with line nodes, and focused especially on the behavior of the finite energy DOS. We found that (1), while at very low temperatures and fields the specific heat anisotropy is in agreement with the Doppler shift analysis, *both* at higher T and low H , *and* at higher H for any T , it changes sign, and exhibits a maximum, rather than a minimum, for \mathbf{H} along a nodal direction; (2) accounted simultaneously for the twofold and fourfold pattern in the angle dependence of the thermal conductivity; and (3) used the approach to resolve a controversy regarding the symmetry of the order parameter in CeCoIn₅ in favor of $d_{x^2-y^2}$ gap. We believe that our approach provides a reliable tool to be used alongside experimental measurements for determination of the nodal directions in novel superconductors.

This work was partly done at KITP with support from NSF Grant No. PHY99-07949; and was also supported by the Board of Regents of Louisiana. We thank P. W. Adams, D. A. Browne, C. Capan, P. J. Hirschfeld, Y. Matsuda, and T. Sakakibara for discussions.

- [1] I. Vekhter *et al.*, Phys. Rev. B **59**, R9023 (1999).
- [2] T. Park *et al.*, Phys. Rev. Lett. **90**, 177001 (2003); K. Deguchi *et al.*, *ibid.* **92**, 047002 (2004).
- [3] H. Aoki *et al.*, J. Phys. Condens. Matter **16**, L13 (2004).
- [4] F. Yu *et al.*, Phys. Rev. Lett. **74**, 5136 (1995); H. Aubin *et al.*, *ibid.* **78**, 2624 (1997).
- [5] K. Izawa *et al.*, Phys. Rev. Lett. **86**, 2653 (2001); **88**, 027002 (2002); **89**, 137006 (2002); **90**, 117001 (2003); T. Watanabe *et al.*, Phys. Rev. B **70**, 184502 (2004).
- [6] K. Izawa *et al.*, Phys. Rev. Lett. **87**, 057002 (2001).
- [7] G. E. Volovik, JETP Lett. **58**, 469 (1993).
- [8] C. Kübert and P. J. Hirschfeld, Phys. Rev. Lett. **80**, 4963 (1998); I. Vekhter and P. J. Hirschfeld, Physica C (Amsterdam) **341–348**, 1947 (2000); P. Thalmeier and K. Maki, Phys. Rev. B **67**, 092510 (2003).
- [9] I. Vekhter and A. Houghton, Phys. Rev. Lett. **83**, 4626 (1999).
- [10] A. C. Durst, A. Vishwanath, and P. A. Lee, Phys. Rev. Lett. **90**, 187002 (2003).
- [11] H. Kusunose, T. Rice, and M. Sigrist, Phys. Rev. B **66**, 214503 (2002); H. Kusunose, *ibid.* **70**, 054509 (2004).
- [12] A. B. Vorontsov and I. Vekhter (unpublished).
- [13] I. A. Luk'yanchuk and V. P. Mineev, Zh. Eksp. Teor. Fiz. **93**, 2045 (1987) [Sov. Phys. JETP **66**, 1168 (1987)].
- [14] H. Adachi *et al.*, Phys. Rev. Lett. **94**, 067007 (2005).
- [15] G. Eilenberger, Z. Phys. **214**, 195 (1968); A. I. Larkin and Y. N. Ovchinnikov, Sov. Phys. JETP **28**, 1200 (1969).
- [16] U. Brandt, W. Pesch, and L. Tewordt, Z. Phys. **201**, 209 (1967); W. Pesch, Z. Phys. B **21**, 263 (1975).
- [17] E. H. Brandt, J. Low Temp. Phys. **24**, 409 (1976).
- [18] H. Won and K. Maki, Phys. Rev. B **53**, 5927 (1996).
- [19] The BPT method gives the correct $H = 0$ limit [20]. However, since averaging over the intervortex distance ($\sim \Lambda$) prior to impurity averaging is allowed only when $\Lambda/l \ll 1$, the approach does break down at low H .
- [20] A. Houghton and I. Vekhter, Phys. Rev. B **57**, 10831 (1998).
- [21] L. Tewordt and D. Fay, Phys. Rev. B **72**, 014502 (2005).
- [22] P. J. Hirschfeld, P. Wölfle, and D. Einzel, Phys. Rev. B **37**, 83 (1988).
- [23] M. J. Graf *et al.*, Phys. Rev. B **53**, 15 147 (1996).
- [24] P. Klimesch and W. Pesch, J. Low Temp. Phys. **32**, 869 (1978).
- [25] We checked that moderate changes in the shape of the Fermi surface and in the scattering rate lead to small quantitative changes in the amplitude of the effects discussed here, but do not alter any of our conclusions [12].
- [26] I. Vekhter, P. J. Hirschfeld, and E. J. Nicol, Phys. Rev. B **64**, 064513 (2001).
- [27] Similar behavior of the residual DOS at $T = 0$ was found in P. Miranović *et al.*, Phys. Rev. B **68**, 052501 (2003); M. Udagawa, Y. Yanase, and M. Ogata, *ibid.* **70**, 184515 (2004), but not separated from the in-plane anisotropy of H_{c2} . We verified that the behavior of $N(0, \mathbf{H})$ is the same for isotropic H_{c2} , and hence is intrinsic.
- [28] The value of T_0 weakly depends on the shape of the Fermi surface and the impurity scattering rate.
- [29] A. Bianchi *et al.*, Phys. Rev. Lett. **91**, 187004 (2003).
- [30] K. Maki, Phys. Rev. **158**, 397 (1967).